J Mol Model (2012) 18:3301–3310
DOI 10.1007/s00894-011-1345-4

ORIGINAL PAPER

Tetraethylorthosilicate as molecular precursor to the formation of amorphous silica networks. A DFT-SCRF study of the base catalyzed hydrolysis

Lorenzo Fernandez · Iñaki Tuñón · Julio Latorre · Carmen Guillem · Aurelio Beltrán · Pedro Amorós

Received: 14 October 2011 / Accepted: 20 December 2011 / Published online: 18 January 2012

Abstract Quantum chemical calculations using density functional theory have been carried out to investigate two chemical pathways for the last step of the hydrolysis of tetraethylorthosilicate (TEOS) in basic catalyzed environment. The two models that are introduced in this study depend on the number of water molecules involved at the base catalyzed hydrolysis. Solution equilibrium geometries of the molecules involved in the transition states, reactants and product complexes of the two chemical pathways were fully optimized at B3LYP level of theory with the standard 6-31+G(d) basis set, modeling solvent effects using a polarizable continuum solvation model (PCM). Both models predict relative low activation energies. However, the model with two water molecules seems to be more adequate to describe the basic hydrolysis. A natural bond orbital (NBO) analysis seems to show that the proton transfer from water to ethoxy group would occur through a large hyperconjugative interaction, $LP_O \rightarrow \sigma^*(O\text{-}H)$, which is related to the nonbonding oxygen lone pair orbital from ethoxy group with the vicinal σ*(O-H) anti bonding orbital O-H of a water molecule.

Keywords DFT · Hydrolysis · SCRF · Potential energy surface · Tetraethylorthosilicate

L. Fernandez (✉) · J. Latorre · C. Guillem · A. Beltrán · P. Amorós
Institut de Ciència dels Materials de la Universitat de Valencia (ICMUV),
P.O. Box 22085, E-46071 Valencia, Spain
e-mail: lorenzo.fernandez@uv.es

I. Tuñón
Department of Quim Fis, Universitat de Valencia,
E-46100 Burjassot, Spain

Introduction

Tetraethylorthosilicate, TEOS (Scheme 1), also named tetraethoxysilane ($Si(OR)_4$ where OR is an ethoxy group, i.e., OCH_2CH_3) is widely utilized in the sol-gel chemistry of alkoxides [1–5] as molecular precursor, where through hydrolysis and condensation reactions, a large variety of silica based materials are produced such as xerogels, aerogels, glass, glass ceramics and composite materials because a useful advantage consists of the fact that once displaced from the metal (or metalloid) environment by solvolysis, alcohol groups do not take part in the subsequent condensation processes and it is easily removed from the solution [6]. Through sol–gel processing, it can be considered that hydrolysis and condensation processes of TEOS lead to the formation of an amorphous silica network due to the fact that TEOS is extremely sensitive to hydrolysis by water [7]. On the other hand, it is known that during most of the hydrothermal synthesis of crystalline aluminosilicate zeolites, the silica sources come mainly from silica gel and sodium silicate. However, an organic silica source as TEOS in the presence of surfactant has been successfully used to synthesize zeolites such as MFI [8], zeolite–beta [9] and MCM-22 [10] and also a mesoporous molecular sieve material, named MCM-41 [11]. It is worth noting that there exists mesoporous silica based materials that can be synthesized in basic conditions using molecular precursors as silatranes [12] obtained from TEOS. The rate of hydrolysis would determine whether a solid network is able to form before or after an ordered mesophase forms. Thence, differences in precursor reactivity can play a significant role in determining the range of conditions in which ordered materials can be synthesized [12, 13].

Some authors [14–16] proposed that the alkoxisilane hydrolysis would involve a S_N2 mechanism. Under base-

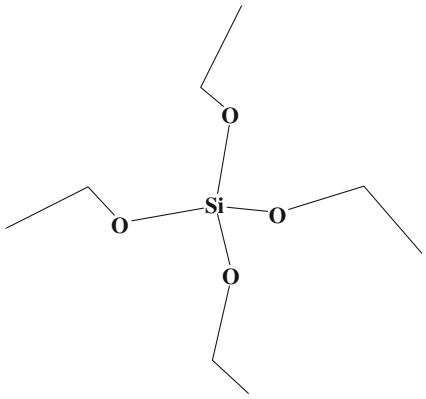

Scheme 1 Tetraethylorthosilicate, TEOS

catalyzed hydrolysis [1], there exists two mechanistic models. In a first model H_2O rapidly dissociates to produce nucleophilic hydroxyl anions. Afterward, according to Iler [14] and Keefer[15], the hydroxyl anion would attack the silicon atom where OH^- displaces the OR^- group with inversion of the silicon tetrahedron (see Scheme 2). In the second model proposed by Pohl et al. [16], there would be a stable five-coordinated intermediate which decays through a second transition state (see Scheme 3). In this way, a complete hydrolysis under basic/acid-catalyzed conditions would occur over a four-step process reaching a $Si(OH)_4$ monomer. It is noteworthy to recall that the experimental pK_a of $Si(OH)_4$ is 9.8 [14]. Afterward, condensation of $Si(OH)_4$ monomers leads to a silica framework.

One of the first experimental studies was achieved by Aelion et al. [7]. They evaluated condensation rate constants by analyzing the kinetic of acid- and alkaline catalyzed hydrolysis of ethyl silicate (TEOS) by volumetric titration. Later, much of the experimental investigations on hydrolysis kinetics applied to alkoxysilanes have been performed by ^{29}Si solution NMR and vibrational spectroscopies such as, mainly FTIR and Raman [17–45]. From the NMR experiments, early detailed kinetic analysis of the rate constants, k_1 to k_4, for the four step processes of TEOS hydrolysis in acid-catalyzed environment have been published [19, 23]. However, quantitative and detailed measurements of basic-catalyzed solution are not yet published. NMR spectroscopy is a powerful instrument to quantify all of the species that are present during hydrolysis because it distinguishes among the different silicon species, enabling measurement of the different hydrolysis and condensation rates for a tetrahedrally coordinated organosilicate. However, there exist some difficulties that are inherent for this technique; indeed, the NMR signal is limited both by low natural abundance and the temporal resolution due to the long ^{29}Si spin-lattice relaxation time (T1). According to Artaki et al. [45], the hydrolysis process of alkoxysilane in an alkaline catalyzed system shows serious phase separation resulting in the great difficulty of following the reaction with a loss of NMR signal. FTIR spectroscopy has a high sensitivity with a fast scanning ability, however, this spectroscopy provided ‘in situ” qualitative data [27]. Recently, it is worth noting that Jiang et al. [38] obtained “in situ” quantitative analysis of methyltriethoxysilane (MTES) hydrolysis by calibrating the system with standards.

Hydrogen bond is one of the weak chemical interactions, and it plays crucial roles in a lot of chemical and biochemical processes. Functional groups as hydroxyls are able to develop intermolecular hydrogen bonding which can influence molecular stability, and also transition states [46] favoring different reaction pathways. This feature is significant for the fourth step process of TEOS hydrolysis in alkaline reactive medium which contain multiple hydroxyl groups capable of extensive intra- and intermolecular hydrogen-bonded networks. The present work reports a theoretical investigation using density functional theory (DFT) methodology in order to understand the fourth step process of TEOS hydrolysis in base catalyzed environment modeling solvent effects using a self-consistent reaction field (SCRF) as the polarizable continuum solvation model (PCM) [47]. In the PCM model, the solute molecules are embedded in molecular-shaped cavities surrounded by a continuous dielectric medium, whose polarization is reproduced by point charges distributed on the cavity surface. PCM exploits cavities built with interlocking spheres centered on atoms, according to the GEnerating POLyhedra (GEPOL) procedure [48]. The objective of this work is to examine theoretical reaction pathways taking into account the intermolecular hydrogen-bonding interactions and thence to deduce an appropriate model. From the results of this study, a new investigation is in progress to complete the theoretical base catalyzed hydrolysis of TEOS occurring over a four-step process and thus to calculate their theoretical hydrolysis rates. As the experimental kinetic data of alkoxysilane hydrolysis in base catalyzed environment are scarce, the theoretical

Scheme 2 Inversion of the silicon tetrahedron

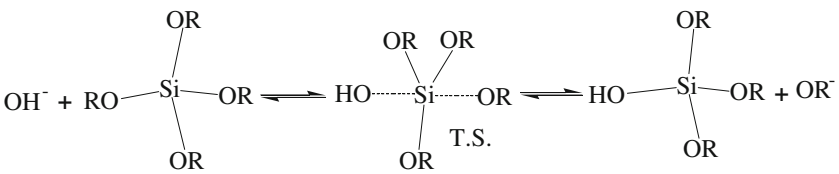

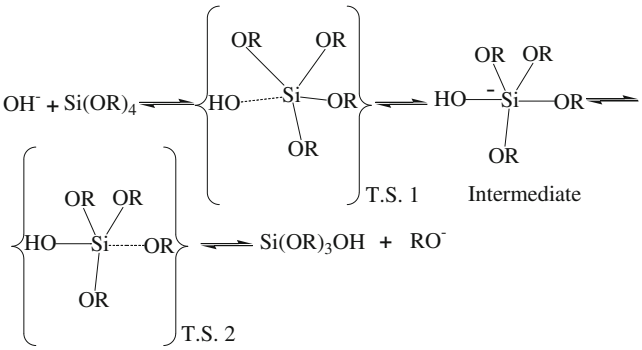

Scheme 3 Second transition state

knowledge of their hydrolysis rates would allow getting a deeper insight on the role precursor reactivity to obtain ordered mesoporous materials.

Calculations

All the calculations on the potential energy surface (PES) and geometry optimizations of the critical points (transition structures, reactants and products) were carried out using a DFT method at the B3LYP [49–51] level of theory with the standard 6-31+G(d) basis set using the Gaussian03 program package [52]. Density functional methods have been quite useful for hydrogen-bonded complexes; in particular the B3YLP functional has been proven to be highly effective with large basis sets [53–56] and the inclusion of diffuse basis functions is indispensable to describe negatively charged systems [57]. Calculations have been performed taking into account the solvent effects using a self-consistent reaction field (SCRF) such as the polarizable continuum solvation model (PCM) [47]. Due to convergence problems during optimization, internal parameters of the program such as TSARE and RMIN were changed. Notwithstanding, once the optimizations of all of the critical points have been obtained, these ones have been newly calculated with identical parameters (RMIN, TSARE, …) in order to harmonize the results. Each solute atom is assigned a Bondi's radii [58]. All calculations in solution have been performed using the dielectric constant of water (78.39). Harmonic vibrational frequencies are computed at this level in order to verify the character of the stationary point located (one imaginary frequency for a TS and none for a minimum) and also to obtain the zero-point energies (ZPE) and contributions to the free energy. In the course of the calculations for each chemical pathway, the transition vector coincides with the true reaction vector at the actual transition state (i.e., the single eigenvector with negative eigenvalue at the saddle point). Furthermore, each transition state has been connected with the corresponding minima on the appropriate potential energy surface by calculating the minimum energy path through the intrinsic reaction coordinate (IRC) [59, 60]. The geometries from the IRC pathway were optimized to obtain the corresponding reactant complex (RC) and product complex (PC). Natural bond orbital (NBO) [61] calculations have also been performed for some conformations using the standard 6-31+G(d) basis set. In this context, a study of hyperconjugative interactions has been completed. Hyperconjugation may be given as a stabilizing effect that arises from an overlap between an occupied orbital with another neighboring electron deficient orbital when these orbitals are properly oriented. This noncovalent bonding-antibonding interaction can be quantitatively described in terms of the NBO approach that is expressed by means of the second-order perturbation interaction energy (E^2) [62–65]. This energy represents the estimate of the off-diagonal NBO Fock matrix elements.

Results and discussion

The first part of this study describes the theoretical mechanism for a base-catalyzed hydrolysis of $Si(OH)_3OR$ ($R=CH_2CH_3$) which is catalyzed by hydroxide ion (OH^-) in the presence of one water molecule and a continuum environment. The second part will considerer the reaction pathway in which the base catalyzed hydrolysis occurs in the presence of two explicit water molecules.

Stationary structures for the first theoretical pathway for a base-catalyzed hydrolysis with one water molecule are presented in Fig. 1. This corresponds to the attack of the hydroxide ion on the electropositive silicon atom to reach protonated silicic monomer, $Si(OH)_4$ and ethanol (CH_3CH_2OH) through three transition states, thus, displaying a theoretical pathway in three steps. The first step corresponds to the nucleophilic attack by OH^- (TS1) and the formation of a neutral pentacoordinated silicon complex (PC1). This mechanism proceeds via a bimolecular nucleophilic substitution (S_N2-Si) process due to the fact that the silicon atom can expand its valence. The transition state (TS1) presents a low imaginary frequency (see Fig. 1). The second step corresponds to the breaking of the Si-OR bond (TS2) with the displacement of ethoxy group, being stabilized by hydrogen bonds with the $Si(OH)_4$ species (PC2). The fully separated fragments $Si(OH)_4$, C_2H_5OH and OH^- are obtained in the third step after a proton transfer from water to the leaving ethoxy group (TS3). Independently of SCRF parameter variations, a full geometry optimization leads to $Si(OH)_3O^-$ complex. In order to prevent the proton transfer the O-H distances of the silicic monomer were fixed. Notwithstanding, full optimizations in gas phase of RC3 and PC3 complexes confirm the last step in Fig. 1,

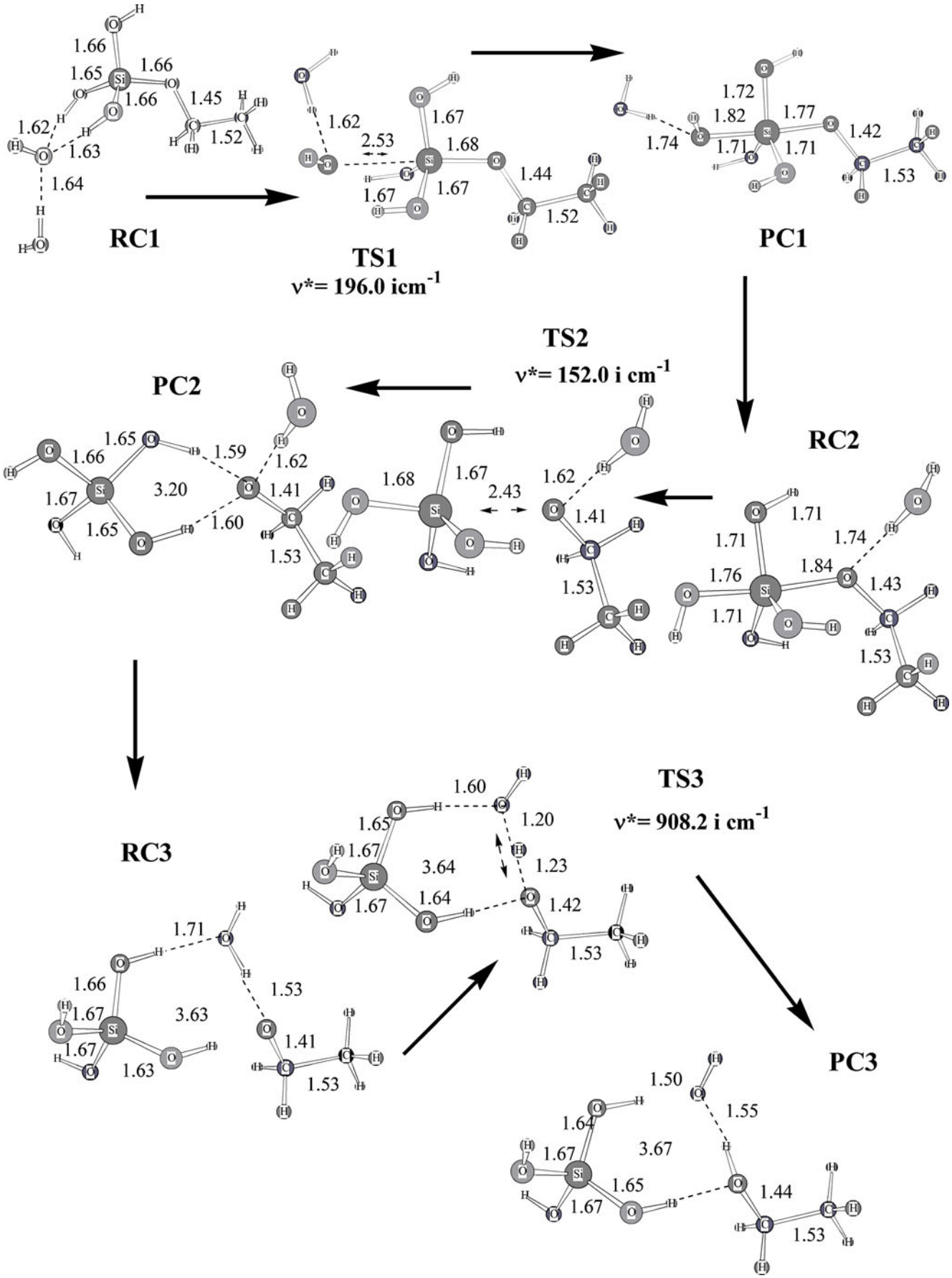
RC1
TS1
ν*= 196.0 icm-1
PC1
TS2
ν*= 152.0 i cm-1
PC2
RC2
RC3
TS3
ν*= 908.2 i cm-1
PC3

◀ **Fig. 1** Geometries for the first theoretical pathway of a base-catalyzed hydrolysis of $Si(OH)_3OR$ ($R=CH_2CH_3$) in the presence of one water molecule. All of the geometries of transition states show the eigenvector corresponding to the imaginary vibration mode that is associated with the reaction coordinate

where no formation of $Si(OH)_3O^-$ complex is obtained.[1] The barrier energies of the first theoretical model are given in Table 1. Free energies have been corrected taking into account the zero point energy. The activation free energy measured from RC1 is 12.58 kcal mol^{-1} while the value from separated reactants is 12.90 kcal mol^{-1}.[2]

The second theoretical pathway considers the presence of two water molecules and the results are presented in Fig. 2 and Table 2. As in the first chemical pathway analyzed above, this second pathway also occurs via three steps. The presence of an additional water molecule modifies the geometries and energetics of the reaction. After the formation of the pentacoordinated complex and the displacement of the ethoxy group, the reaction continues up to an intermediate complexe (PC1=RC2), which through an intermolecular proton transfer (TS3) process allows to obtain the final products of the base catalyzed hydrolysis of TEOS. In this case it was not necessary to fix the OH distances in order to prevent the formation of $Si(OH)_3O^-$ anion. Thence, the two theoretical models conclude to identical final products: $Si(OH)_4$ ethanol and OH^-, although geometrical restrictions were needed in the model containing only one water molecule. This difference is probably related to the limitations of the continuum model to provide an adequate stabilization of small charged species and points out to the two-solvent molecules as the most adequate to analyze the process. The details of corrected energies with ZPE from the conformations in Fig. 2 are presented in Table 2 where the activation free energy measured from RC1 is 10.28 kcal mol^{-1} while from separated reactants is 13.99 kcal mol^{-1}.

A natural bond orbital (NBO) analysis has been performed to provide insight into the role of electronic delocalization in the two chemical pathways. Indeed, a study showed that the hyperconjugative interactions might influence the GIAO calculations in alkoxysilanes such as silatranes [66]. In this way, we have undertaken NBO analysis to the RC3 conformation in Fig. 1, and the PC2=RC3

[1] The SCRF methodology reveals one negative frequency for the energy minimum in the RC1, PC1, RC3 and PC3 complexes. All of them are low, corresponding to the movement of OH bond in H2O molecule or the rotation of CH3 group. In this way, a second low negative frequency appears in the TS3 calculation. No negative frequencies have been obtained from the calculations in gas phase what could confirm these ones as theoretical artifacts from the SCRF methodology.

[2] The conversion of solvation free energies at 298K to a standard state 1M is performed by adding +1.89kcalmol^{-1} to the computed solvation free energy.

Table 1 Total free energy in solution (in hartrees) and their differences (in kcal mol^{-1}, parentheses) relative to those of reactant complex for a base-catalyzed hydrolysis in the presence of one water molecule. Energies have been calculated taking into account the zero point energy (ZPE). To convert solvation free energies at 298 K to a standard state 1 M then +1.89 kcal mol^{-1} must add to the computed solvation free energy

$OH^-...H_2O + Si(OH)_3OR$	RC1	TS1	PC1	RC2	TS2	PC2	RC3	TS3	PC3
−152.361151	−823.810781	−823.790731	−823.801034	−823.796442	−823.792246	−823.809713	−823.833198	−823.817925	−823.834174
−671.450141	(0)	(12.58)	(6.12)	(9.00)	(11.63)	(0.67)	(−14.07)	(−4.48)	(−14.68)
−823.811292									
(−0.32)									

Underlined values are the sum of the total free energy in solution (in hartrees) for all of complexes

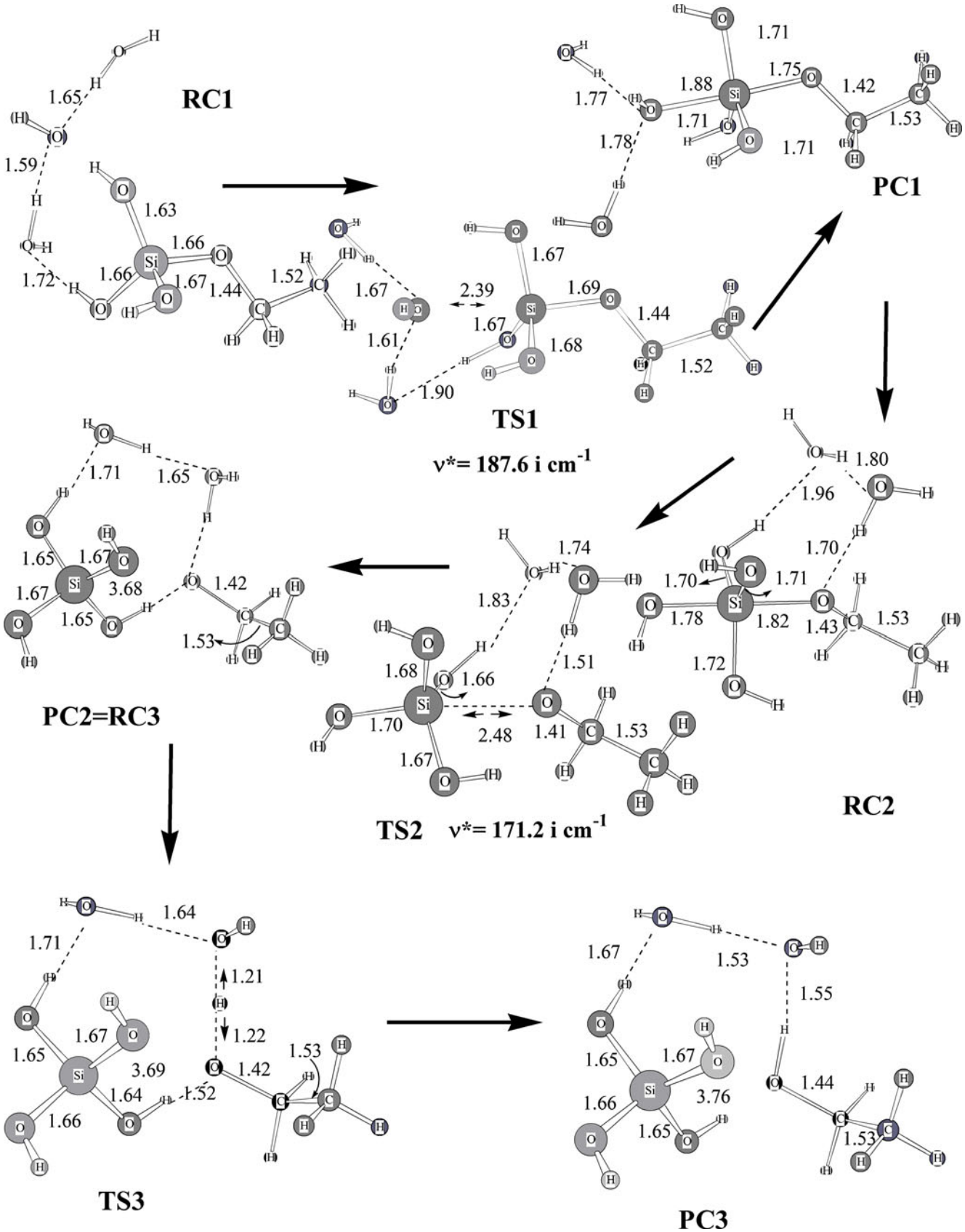
RC1
PC1
TS1
ν*= 187.6 i cm-1
PC2=RC3
RC2
TS2 ν*= 171.2 i cm-1
TS3
PC3

◀ **Fig. 2** Geometries for the second theoretical pathway of a base-catalyzed hydrolysis of $Si(OH)_3OR$ ($R=CH_2CH_3$) in the presence of two water molecules. All of the geometries of transition states show the eigenvector corresponding to the imaginary vibration mode that is associated with the reaction coordinate

intermediate in Fig. 2. All of these structures correspond to complexes just before the proton transfer. NBO calculations applied to RC3 conformation in Fig. 1 reports that the more intense magnitudes for the hyperconjugative interactions are related to the nonbonding oxygen lone pair orbital from OR^- (ethoxy group) with the vicinal σ*(O-H) anti bonding orbital O-H from $Si(OH)_4$ where $LP_O \rightarrow \sigma^*(O\text{-}H)$ is 66.90 kcal mol^{-1} and also to the nonbonding oxygen lone pair orbital from OR^- (ethoxy group) with the vicinal σ*(O-H) anti bonding orbital O-H from water molecule with $LP_O \rightarrow \sigma^*(O\text{-}H)$ is 50.62 kcal mol^{-1}. The third interaction, $LP_O \rightarrow \sigma^*(O\text{-}H)$, with an energy of 28.82 kcal mol^{-1} is related to the nonbonding oxygen lone pair orbital from water molecule with the vicinal σ*(O-H) anti bonding orbital O-H from $Si(OH)_4$. The magnitudes of the hyperconjugative interactions emphasize the fact to fix the OH distance to prevent the proton transfer from $Si(OH)_4$ to ethoxy group and thus to form $Si(OH)_3O^-$ complex. The calculations of the transition state (TS3) unambiguously shows that the proton transfer comes from water molecules. The PC2=RC3 intermediate in Fig. 2 is the second pre-reaction complex that has been studied. Anew, the same behavior is confirmed. The most intense interaction ($LP_O \rightarrow \sigma^*(O\text{-}H)$) gives 103.25 kcal mol^{-1} where the vicinal σ*(O-H) anti bonding orbital O-H comes from the water molecule close to the oxygen of OR^-. The second more intense energy (52.36 kcal mol^{-1}) is associated with the nonbonding oxygen lone pair orbital from OR^- with the vicinal σ*(O-H) anti bonding orbital O-H from $Si(OH)_4$, however, its magnitude remains much less intense than the interaction with the anti bonding orbital O-H from water molecule. The magnitude of the others interactions are below 9.01 kcal mol^{-1}. The results of NBO calculations would seem to indicate that an intense $LP_O \rightarrow \sigma^*(O\text{-}H)$ plays an important role and it shows that the lone pairs which are formally nonbonding in the pre-reaction complexes prior to intermolecular hydrogen atom transfer, become partially bonding in TS structures.

Comparison of the free energy barriers and of the geometrical description of the reaction mechanisms obtained with the two models points out that the second pathway with two water molecules not only more plausible from the energetic point of view but also a more adequate and consistent theoretical model to study this reaction. In any case both models agree in the fact that the rate limiting step would be the nucleophilic attack of the hydroxide anion to produce the pentacoordinated intermediate. The energetics of this step would be dominated by the desolvation of the nucleophile. A gas phase theoretical study on hydrolysis in acid/base conditions of another silane such as methylmethoxydihydroxysilane has been examined using B3LYP/6-31G(d)(SCRF)//RHF/6-31G(d) in order to determine how many water molecules are involved during both nucleophilic attacks to the silicon center and proton relay for the exchange of covalent and hydrogen bond [46]. Under basic conditions, a hydroxide ion was employed as nucleophile with one water molecule. In this chemical pathway, after a back-side attack, formation of a pentacoordinate intermediate was found. The final reaction product was composed by $MeSi(OH)_2O^-(H_2O)$ and MeOH in which an intermolecular hydrogen bond was established between H_2O and $MeSi(OH)_2O^-$. The estimation of the activation energy for this reaction pathway was 8.1 kcal mol^{-1}. Note that though the silane is different, the order of magnitude for this activation energy is close to that obtained with our second model. Unfortunately, only the study under acid and neutral conditions varying the size of water clusters (dimer, trimer etc.) has been reported [46]. The analysis of the results indicates that the activation energy decreases with the number of water molecules. According to Okumoto et al. [46], two water molecules

Table 2 Total free energy in solution (in hartrees) and their differences (in kcal mol^{-1}, parentheses) relative to those of reactant complex for a base-catalyzed hydrolysis in the presence of two water molecules. Energies have been calculated taking into account the zero point energy (ZPE). To convert solvation free energies at 298 K to a standard state 1 M then +1.89 kcal mol^{-1} must add to the computed solvation free energy

$OH^-….2H_2O + Si(OH)_3OR$	RC1	TS1	PC1	RC2	TS2	PC2≈RC3	TS3	PC3
−228.769148	−900.213373	−900.196991	−900.200294	−900.190971	−900.182167	−900.22245	−900.212708	−900.213324
−671.450141	(0)	(10.28)	(8.21)	(14.06)	(19.58)	(−5.70)	(0.42)	(0.03)
−900.219289								
(−3.71)								

Underlined values are the sum of the total free energy in solution (in hartrees) for all complexes.

are needed to promote proton transfer. Liu et al. [67] calculated the acid dissociation mechanisms of $Si(OH)_4$ by using Car–Parrinello molecular dynamics simulations in which the reaction involves more than four water molecules. An experimental study [43] on the effect of water content claims that in systems with high water content ($[H_2O]/[TEOS]$), hydrolysis proceeds up to completion, while in systems with a low water content hydrolysis is incomplete. Our second model would then be in agreement with this experimental study. Up to now, only one global experimental activation energy for the complete base-catalyzed hydrolysis of TEOS has been published, providing a value of about 6 kcal mol^{-1} [43, 44] in qualitative agreement with our theoretical estimations.

Conclusions

Tetraethylorthosilicate (TEOS) is one of the more important molecular precursors in the sol-gel chemistry of alkoxides and it takes part in the synthesis of some zeolites and mesoporous molecular sieve materials. Detailed hydrolysis of TEOS in acid catalyzed environment has been experimentally studied, however, the equivalent study in basic conditions is still lacking. In this way, a theoretical study on the hydrolysis is proposed which is mainly centered in the last step process because the presence of multiple hydrogen bonds can influence molecular stability and transition states. The present theoretical investigation has been performed using DFT methodology to understand TEOS hydrolysis in a base catalyzed environment modeling solvent effects using a self-consistent reaction field (SCRF) as the polarizable continuum solvation model (PCM). Calculation of the potential energy surface (PES) and optimizations of stationary states at the B3LYP level of theory with the standard 6-31+G(d) basis set have allowed us to explore two chemical pathway depending on the number of water molecules explicitly considered during hydrolysis of TEOS. The first model considers one water molecule whereas the second one is performed with two explicit water molecules. Both models predict low activation energies. The comparison of the theoretical models shows that the second model is more plausible. A natural bond orbital (NBO) analysis has been performed on the two chemical pathways where it would seem that the proton transfer from water to ethoxy group occurs through the more intense magnitude of the hyperconjugative interaction, $LP_O \rightarrow \sigma^*(O\text{-}H)$, that is related to the nonbonding oxygen lone pair orbital from ethoxy group with the vicinal σ*(O-H) anti bonding orbital O-H from water molecule.

Acknowledgments This research was supported by the Generalitat Valenciana (GV2008-122). Lorenzo Fernandez was supported by the Ramon y Cajal program by the Ministry of Science and Technology from Spain.

References

1. Brinker CJ, Scherer GW (1990) Sol-gel science. The physics and chemistry of sol-gel processing. Academic, Dordrecht
2. Hench LL, West JK (1990) The Sol-Gel Process. Chem Rev 90:33–72
3. Livage J, Sanchez C (1992) Sol-gel chemistry. J Non-Cryst Solids 145:11–19
4. Sanchez C, Livage J (1990) Sol-gel chemistry from metal alkoxide precursors. New J Chem 14:513–521
5. Novak BM (1993) Hybrid nanocomposite materials - between inorganic glasses and organic polymers. Adv Mater 5:422–433
6. Sanchez C, Livage J, Henry M, Babonneau F (1988) Chemical modification of alkoxide precursors. J Non-Cryst Solids 100:65–76
7. Aelion R, Loebel A, Eirich F (1950) Hydrolysis of ethyl silicate. J Am Chem Soc 72:5705–5712
8. Kirschhock CEA, Ravishankar R, Verspeurt F, Grobet PJ, Jacobs PA, Martens JA (1999) Identification of precursor species in the formation of MFI zeolite in the TPAOH-TEOS-H2O system. J Phys Chem B 103:4965–4971
9. Corma A, Gomez V, Martinez A (1994) Zeolite-beta as a catalyst for alkylation of isobutane with 2-butene - influence of synthesis conditions and process variables. Appl Catal A Gen 119:83–96
10. Wu YJ, Ren XQ, Lu YD, Wang J (2008) Rapid synthesis of zeolite MCM-22 by acid-catalyzed hydrolysis of tetraethylorthosilicate. Mater Lett 62:317–319
11. Kresge CT, Leonowicz ME, Roth WJ, Vartuli JC, Beck JS (1992) Ordered mesoporous molecular-sieves synthesized by a liquid-crystal template mechanism. Nature 359:710–712
12. Cabrera S, El Haskouri J, Guillem C, Latorre J, Beltran-Porter A, Beltran-Porter D, Marcos MD, Amoros P (2000) Generalised syntheses of ordered mesoporous oxides: the atrane route. Solid State Sci 2:405–420
13. Bao XY, Li X, Zhao XS (2006) Synthesis of large-pore methylene-bridged periodic mesoporous organosilicas and its implications. J Phys Chem B 110:2656–2661
14. Iler RK (1979) The chemistry of Silica. Wiley, New York
15. Keefer K (1984) In: Brinker CJ, Clark D, Ulrich D (eds) Better Ceramics Through Chemistry. Elsevier, Dordrecht, pp 15–24
16. Pohl E, Osterholtz F (1985) Molecular characterization of composite interfaces. In: Ishida H, Kuma G (eds) Plenum, New York, p 157
17. Kelts LW, Effinger NJ, Melpolder SM (1986) Sol-gel chemistry studied by H-1 And Si-29 nuclear-magnetic-resonance. J Non-Cryst Solids 83:353–374
18. Smith KA (1986) A study of the hydrolysis of methoxysilanes in a 2-phase system. J Org Chem 51:3827–3830
19. Pouxviel JC, Boilot JP (1987) Kinetic simulations and mechanisms of the sol-gel polymerization. J Non-Cryst Solids 94:374–386
20. Kinrade SD, Swaddle TW (1988) Si-29 NMR-studies of aqueous silicate solutions.2. Transverse Si-29 relaxation and the kinetics and mechanism of silicate polymerization. Inorg Chem 27:4259–4264
21. Leyden DE, Atwater JB (1991) Hydrolysis and condensation of alkoxysilanes investigated by internal-reflection Ftir spectroscopy. J Adhes Sci Technol 5:815–829
22. Vanbeek JJ, Seykens D, Jansen JBH (1992) Si-29 NMR monitoring and kinetic modeling of an acid-catalyzed Tmos sol-gel system with molar H2O/Si=8. J Non-Cryst Solids 146:111–120

23. Fyfe CA, Aroca PP (1995) Quantitative Kinetic-Analysis By High-Resolution Si-29 Nmr-Spectroscopy Of The Initial-Stages In The Sol-Gel Formation Of Silica-Gel From Tetraethoxysilane. Chem Mater 7:1800–1806
24. Alam TM, Assink RA, Loy DA (1996) Hydrolysis and esterification in organically modified alkoxysilanes: A Si-29 NMR investigation of methyltrimethoxysilane. Chem Mater 8:2366–2374
25. Sanchez J, Rankin SE, McCormick AV (1996) Si-29 NMR kinetic study of tetraethoxysilane and ethyl-substituted ethoxysilane polymerization in acidic conditions. Ind Eng Chem Res 35:117–129
26. Riegel B, Blittersdorf S, Kiefer W, Hofacker S, Muller M, Schottner G (1998) Kinetic investigations of hydrolysis and condensation of the glycidoxypropyltrimethoxysilane/aminopropyltriethoxy-silane system by means of FT-Raman spectroscopy I. J Non-Cryst Solids 226:76–84
27. Tejedor-Tejedor MI, Paredes L, Anderson MA (1998) Evaluation of ATR-FTIR spectroscopy as an “in situ” tool for following the hydrolysis and condensation of alkoxysilanes under rich H2O conditions. Chem Mater 10:3410–3421
28. Lindberg R, Sundholm G, Oye G, Sjoblom J (1998) A new method for following the kinetics of the hydrolysis and condensation of silanes. Colloids Surf A Physicochem Eng Asp 135:53–58
29. Rankin SE, Sefcik J, McCormick AV (1999) Similarities in the hydrolysis pseudoequilibrium behavior of methyl-substituted ethoxysilanes. Ind Eng Chem Res 38:3191–3198
30. Rankin SE, Sefcik J, McCormick AV (1999) Trimethylethoxysilane liquid-phase hydrolysis equilibrium and dimerization kinetics: catalyst, nonideal mixing, and the condensation route. J Phys Chem A 103:4233–4241
31. Rankin SE, McCormick AV (1999) Si-29 NMR study of base-catalyzed polymerization of dimethyldiethoxysilane. Magn Reson Chem 37:S27–S37
32. Kim MT (2000) Deposition kinetics of silicon dioxide from tetraethylorthosilicate by PECVD. Thin Solid Films 360:60–68
33. Karmakar B, De GT, Ganguli D (2000) Dense silica microspheres from organic and inorganic acid hydrolysis of TEOS. J Non-Cryst Solids 272:119–126
34. Donatti DA, Vollet DR, Ruiz AI (2003) Calorimetric study of the effect of water quantity on tetramethoxysilane hydrolysis under ultrasound stimulation. J Phys Chem B 107:3091–3094
35. Delak KM, Farrar TC, Sahai N (2005) Si-29 NMR sensitivity enhancement methods for the quantitative study of organosilicate hydrolysis and condensation. J Non-Cryst Solids 351:2244–2250
36. Jiang HM, Zheng Z, Li ZM, Wang XL (2006) Effects of temperature and solvent on the hydrolysis of alkoxysilane under alkaline conditions. Ind Eng Chem Res 45:8617–8622
37. Jiang HM, Zheng Z, Xiong JW, Wang XL (2007) Studies on dialkoxysilane hydrolysis kinetics under alkaline conditions. J Non-Cryst Solids 353:4178–4185
38. Jiang H, Zheng Z, Wang X (2008) Kinetic study of methyltriethoxysilane (MTES) hydrolysis by FTIR spectroscopy under different temperatures and solvents. Vib Spectrosc 46:1–7
39. Mazur M, Mlynarik V, Valko M, Pelikan P (1999) The time evolution of the sol-gel process: Si-29 NMR study of hydrolysis and condensation reactions of tetramethoxysilane. Appl Magn Reson 16:547–557
40. Harris MT, Brunson RR, Byers CH (1990) The base-catalyzed-hydrolysis and condensation-reactions of dilute and concentrated Teos solutions. J Non-Cryst Solids 121:397–403
41. Cihlar J (1993) Hydrolysis and polycondensation of ethyl silicates.1. Effect of Ph and catalyst on the hydrolysis and polycondensation of tetraethoxysilane (Teos). Colloid Surf A Physicochem Eng Asp 70:239–251
42. Liu RL, Xu X, Wu D, Sun YH, Gao HC, Yuan HZ, Deng F (2004) Comparative study on the hydrolysis kinetics of substituted ethoxysilanes by liquid-state Si-29 NMR. J Non-Cryst Solids 343:61–70
43. Sefcik J, McCormick AV (1997) Kinetic and thermodynamic issues in the early stages of sol-gel processes using silicon alkoxides. Catal Today 35:205–223
44. Yoon H-S, Park H-S, Kim S-H (1994) A kinetic study on the hydrolysis and condensation of TEOS in basic condition by sol-gel method. Hwahak Konghak 32:557–565
45. Artaki I, Bradley M, Zerda TW, Jonas J (1985) Nmr and raman-study of the hydrolysis reaction in sol-gel processes. J Phys Chem 89:4399–4404
46. Okumoto S, Fujita N, Yamabe S (1998) Theoretical study of hydrolysis and condensation of silicon alkoxides. J Phys Chem A 102:3991–3998
47. Cossi M, Barone V, Cammi R, Tomasi J (1996) Ab initio study of solvated molecules: a new implementation of the polarizable continuum model. Chem Phys Lett 255:327–335
48. Pascual-ahuir JL, Silla E, Tuñón I (1994) Gepol - an improved description of molecular-surfaces.3. A new algorithm for the computation of a solvent-excluding surface. J Comput Chem 15:1127–1138
49. Becke AD (1993) Density-functional thermochemistry.3. The role of exact exchange. J Chem Phys 98:5648–5652
50. Lee CT, Yang WT, Parr RG (1988) Development of the Colle-Salvetti correlation-energy formula into a functional of the electron-density. Phys Rev B: Condens Matter 37:785–789
51. Miehlich B, Savin A, Stoll H, Preuss H (1989) Results obtained with the correlation-energy density functionals of Becke and Lee, Yang and Parr. Chem Phys Lett 157:200–206
52. Frisch MJ, Trucks GW, Schlegel HB, Scuseria GE, Robb MA, Cheeseman JR, Montgomery JA, Vreven T, Kudin KN, Burant JC, Millam JM, Iyengar SS, Tomasi J, Barone V, Mennucci B, Cossi M, Scalmani G, Rega N, Petersson GA, Nakatsuji H, Hada M, Ehara M, Toyota K, Fukuda R, Hasegawa J, Ishida M, Nakajima T, Honda Y, Kitao O, Nakai H, Klene M, Li X, Knox JE, Hratchian HP, Cross JB, Bakken V, Adamo C, Jaramillo J, Gomperts R, Stratmann RE, Yazyev O, Austin AJ, Cammi R, Pomelli C, Ochterski JW, Ayala PY, Morokuma K, Voth GA, Salvador P, Dannenberg JJ, Zakrzewski VG, Dapprich S, Daniels AD, Strain MC, Farkas O, Malick DK, Rabuck AD, Raghavachari K, Foresman JB, Ortiz JV, Cui Q, Baboul AG, Clifford S, Cioslowski J, Stefanov BB, Liu G, Liashenko A, Piskorz P, Komaromi I, Martin RL, Fox DJ, Keith T, Al-Laham MA, Peng CY, Nanayakkara A, Challacombe M, Gill PMW, Johnson B, Chen W, Wong MW, Gonzalez C, Pople JA (2004) Gaussian 03, Revision C.02. Gaussian Inc, Wallingford
53. Rablen PR, Lockman JW, Jorgensen WL (1998) Ab initio study of hydrogen-bonded complexes of small organic molecules with water. J Phys Chem A 102:3782–3797
54. Gonzalez L, Mo O, Yanez M (1999) Density functional theory study on ethanol dimers and cyclic ethanol trimers. J Chem Phys 111:3855–3861
55. Tsuzuki S, Houjou H, Nagawa Y, Goto M, Hiratani K (2001) Cooperative enhancement of water binding to crownophane by multiple hydrogen bonds: analysis by high level ab initio calculations. J Am Chem Soc 123:4255–4258
56. Zhang Q, Bell R, Truong TN (1995) Ab-initio and density-functional theory studies of proton-transfer reactions in multiple hydrogen-bond systems. J Phys Chem 99:592–599
57. Clark T, Chandrasekhar J, Spitznagel GW, Schleyer PV (1983) Efficient diffuse function-augmented basis-sets for anion calculations.3. The 3-21+G basis set for 1st-row elements, Li-F. J Comput Chem 4:294–301
58. Bondi A (1964) Van Der Waals volumes + radii. J Phys Chem 68:441–451
59. Gonzalez C, Schlegel HB (1989) An improved algorithm for reaction-path following. J Chem Phys 90:2154–2161
60. Fukui K (1981) The path of chemical-reactions - the Irc approach. Acc Chem Res 14:363–368

61. Reed AE, Curtiss LA, Weinhold F (1988) Intermolecular interactions from a natural bond orbital, donor-acceptor viewpoint. Chem Rev 88:899–926
62. Reed AE, Weinhold F (1985) Natural localized molecular-orbitals. J Chem Phys 83:1736–1740
63. Reed AE, Weinstock RB, Weinhold F (1985) Natural-population analysis. J Chem Phys 83:735–746
64. Reed AE, Weinhold F (1983) Natural bond orbital analysis of near-Hartree-Fock water dimer. J Chem Phys 78:4066–4073
65. Foster JP, Weinhold F (1980) Natural Hybrid Orbitals. J Am Chem Soc 102:7211–7218
66. Fernandez L, Viruela-Martin P, Latorre J, Guillem C, Beltrán A, Amorós P (2007) Molecular precursors of mesostructured silica materials in the atrane route. A DFT/GIAO/NBO theoretical study. J Mol Struct THEOCHEM 822:89–102
67. Liu XD, Lu XC, Meijer EJ, Wang RC, Zhou HQ (2010) Acid dissociation mechanisms of Si(OH)(4) and Al(H(2)O)(6)(3+) in aqueous solution. Geochim Cosmochim Acta 74:510–516